Structure of Wedge-Induced Oblique Detonations with Small Heat Release

Daniel Martínez-Ruiz[1], César Huete[2], Antonio L. Sánchez[3], Forman A. Wiliams[3]
[1]Depto. de Mec. de Fluidos y Prop. Aeroespacial, UPM, 28040, Madrid, España
[2]Depto. de Ing. Térmica y de Fluidos, Univ. Carlos III de Madrid, 28911, Leganés, España
[3]MAE, University of California San Diego, La Jolla CA, USA.

1 Introduction

Oblique detonations are ubiquitous in supersonic propulsion applications [1]. The strong nonlinear character of the flow hinders associated experimental and computational investigations. As a result, despite significant research efforts, many aspects of the formation, dynamics, and stability of oblique detonations remain unclear. Simplified models can be instrumental in understanding the complicated physicochemical interactions that determine the detonation response. The present work exploits simplifications arising in weakly exothermic detonations when the post-shock conditions are supersonic, leading to a compact formulation involving ordinary differential equations to be integrated along prescribed characteristic lines. The resulting formulation, similar to that used recently to analyze diffusion-flame ignition by impingement of a shock wave on a mixing layer [2, 3], can be used to investigate a wide range of oblique-detonation problems involving finite-rate effects, and is used here to investigate the structure of wedge-induced oblique detonations [4].

2 Jump conditions across oblique detonations

The well-known ZND structure of oblique detonations, schematically represented in Fig. 1, involves a leading shock wave followed by a reaction region. In the notation employed, flow properties upstream from the shock will be denoted by the subscript u, whereas the subscript o will be used for the gas state immediately downstream from the shock and the subscript b will be used for the final equilibrium burnt-gas properties. For an oblique detonation with incident angle σ and incident Mach number M_u the changes in density ρ, pressure p, temperature T, and Mach number M from the upstream values as well as the counterclockwise flow deflection ν can be computed with use made of the Rankine-Hugoniot equations [5]. The conditions immediately behind the chemically-frozen shock are given by the simplified equations

$$\frac{\rho_o}{\rho_u} = F_\rho(M_u, \sigma) = \frac{(\gamma+1)M_u^2 \sin^2\sigma}{(\gamma-1)M_u^2\sin^2\sigma + 2}, \tag{1}$$

$$\frac{p_o}{p_u} = F_p(M_u, \sigma) = \frac{2\gamma M_u^2 \sin^2\sigma + 1 - \gamma}{\gamma+1}, \tag{2}$$

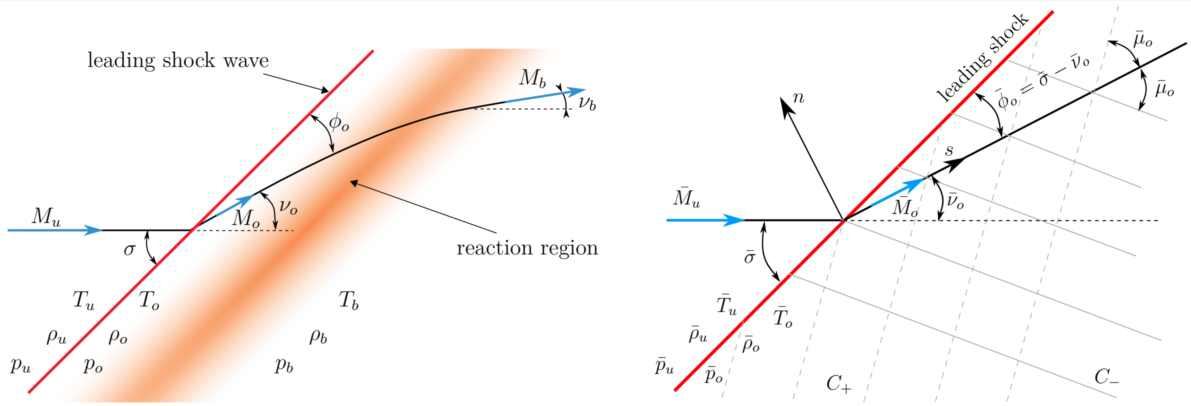

Figure 1: Schematic view of the jump conditions across an oblique shock, and coordinate system and characteristic lines of the flow.

$$\frac{T_o}{T_u} = F_T(M_u,\sigma) = \frac{[2\gamma M_u^2\sin^2\sigma + 1 - \gamma][(\gamma-1)M_u^2\sin^2\sigma + 2]}{(\gamma+1)^2 M_u^2 \sin^2\sigma}, \tag{3}$$

$$M_o = F_M(M_u,\sigma) = \frac{1}{\sin\phi_o}\left[\frac{2+(\gamma-1)M_u^2\sin^2\sigma}{2\gamma M_u^2\sin^2\sigma + 1 - \gamma}\right]^{1/2}, \tag{4}$$

$$\nu_o = F_\nu(M_u,\sigma) = \tan^{-1}\left\{\frac{2(M_u^2\sin^2\sigma - 1)\cot\sigma}{2 + M_u^2[\gamma + \cos(2\sigma)]}\right\}, \tag{5}$$

where γ is the specific-heat ratio, and the angle $\phi_o = \sigma - \nu_o$ appearing in Eq. (4) measures the inclination of the post-shock stream with respect to the shock. For weakly exothermic detonations with small heat release per unit mass of gas mixture Q the relative variations of all flow properties across the reaction region and the associated deflection of the streamlines are small, as can be seen by the linearized relations

$$-\frac{\rho_b - \rho_o}{\rho_o} = -\frac{(p_b - p_o)/p_o}{\gamma M_o^2 \sin^2\phi_o} = \frac{(T_b - T_o)/T_o}{1 - \gamma M_o^2\sin^2\phi_o} = \frac{\nu_o - \nu_b}{\cos\phi_o \sin\phi_o} = \frac{Q/(c_p T_o)}{1 - M_o^2\sin^2\phi_o}. \tag{6}$$

of order $q = Q/(c_p T_o) \ll 1$, where c_p is the specific heat at constant pressure.

3 Reduced Formulation for Small Heat Release

Equations will be written for the small flow departures from a predetermined base flow, defined by the constant incident angle $\bar{\sigma}$ and the upstream values of the Mach number $\bar{M}_u$, pressure $\bar{p}_u$, temperature $\bar{T}_u$, and density $\bar{\rho}_u$. Corresponding post-shock properties for this base solution are given, in terms of Eqs. (1)–(5), by

$$\frac{\bar{T}_o}{\bar{T}_u} = F_T(\bar{M}_u,\bar{\sigma}), \quad \frac{\bar{p}_o}{\bar{p}_u} = F_p(\bar{M}_u,\bar{\sigma}), \quad \frac{\bar{\rho}_o}{\bar{\rho}_u} = F_\rho(\bar{M}_u,\bar{\sigma}), \quad \bar{M}_o = F_M(\bar{M}_u,\bar{\sigma}), \quad \bar{\nu}_o = F_\nu(\bar{M}_u,\bar{\sigma}) \tag{7}$$

The post-shock velocity can be evaluated in terms of $\bar{M}_o$ and $\bar{T}_o$ with use made of $\bar{U}_o = \bar{M}_o((\gamma-1)c_p\bar{T}_o)^{1/2}$. Since the flow deflection across the reaction region is small, the streamlines are almost exactly aligned with the post-shock unperturbed flow, thereby motivating the use of the cartesian coordinate system of Fig. 1, with the streamwise coordinate s and the transverse coordinate n scaled with the induction length $\bar{U}_o t_i$ based on the characteristic induction time t_i at temperature $\bar{T}_o$. The origin of the reference frame lies at the leading shock. The associated streamwise and transverse velocity components will be denoted by U and V, with the latter related to the flow deflection by $V/\bar{U}_o = \nu - \bar{\nu}_o$. In the limit $q \ll 1$, the chemical reaction results in small relative variations of the different flow variables, which can be described with the linearized form of the governing equations, including the continuity, momentum, and energy conservation equations

$$\frac{\partial \hat{\rho}}{\partial s} + \frac{\partial \hat{U}}{\partial s} + \frac{\partial \hat{V}}{\partial n} = 0 \tag{8}$$

$$\gamma \bar{M}_o^2 \frac{\partial \hat{U}}{\partial s} + \frac{\partial \hat{p}}{\partial s} = 0 \tag{9}$$

$$\gamma \bar{M}_o^2 \frac{\partial \hat{V}}{\partial s} + \frac{\partial \hat{p}}{\partial n} = 0 \tag{10}$$

$$\frac{\partial \hat{T}}{\partial s} - \frac{\gamma - 1}{\gamma}\frac{\partial \hat{p}}{\partial s} = \Omega, \tag{11}$$

written in terms of the dimensionless order-unity perturbation variables

$$\hat{\rho} = \frac{(\rho - \bar{\rho}_o)/\bar{\rho}_o}{q}, \hat{p} = \frac{(p - \bar{p}_o)/\bar{p}_o}{q}, \hat{T} = \frac{(T - \bar{T}_o)/\bar{T}_o}{q}, \hat{U} = \frac{(U - \bar{U}_o)/\bar{U}_o}{q}, \text{ and } \hat{V} = \frac{V/\bar{U}_o}{q}. \tag{12}$$

The above equations must be supplemented with the equation of state written in the linearized form

$$\hat{p} = \hat{\rho} + \hat{T}, \tag{13}$$

considering constant mean molecular weight, an appropriate simplification for reactant mixtures satisfying $q \ll 1$. The problem is simplified by eliminating $\hat{U}$ and $\hat{\rho}$ with use made of Eqs. (8), (9), and (13) to give

$$\frac{\gamma \bar{M}_o^2 - 1}{\gamma \bar{M}_o^2}\frac{\partial \hat{p}}{\partial s} - \frac{\partial \hat{T}}{\partial s} + \frac{\partial \hat{V}}{\partial n} = 0. \tag{14}$$

Besides, since the dimensionless heat-release rate Ω (scaled with $\bar{\rho}_o Q/t_i$) depends on the local composition, the solution requires simultaneous integration of the evolution of species along the streamlines $n =$ constant,

$$\frac{\partial Y_i}{\partial s} = -\omega_i/(\bar{\rho}_o/t_i), \tag{15}$$

where Y_i and $\omega_i(\hat{T}, Y_i)$ are the mass fraction and the mass consumption rate of chemical species i. For a chemically-frozen shock, the boundary conditions at the shock reduce to the upstream mass fractions Y_{i_u} in the incoming stream. While the formulation is compatible with detailed chemical-kinetic mechanisms, a simple irreversible Arrhenius reaction that releases an amount of heat Q per unit mass of gas mixture suffices in many cases to describe the nonlinear effects associated with the strong temperature sensitivity of the reaction,

$$\omega = \rho B Y \exp\left(-\frac{E_a}{R^o T}\right), \tag{16}$$

in terms of the density ρ, temperature T, and reactant mass fraction Y. Here B is a preexponential factor, R^o is the universal gas constant, and E_a is the activation energy. The following description considers the particular case of large values of the dimensionless activation energy such that

$$\frac{E_a}{R^o \bar{T}_o} \sim q^{-1} \gg 1, \tag{17}$$

for which temperature variations of order q result in reaction-rate changes of order unity. In writing the temperature dependence of the reaction rate use is made of the familiar Frank-Kamenetskii linearization involving the reduced activation energy $\beta = (E_a/R^o\bar{T}_o)(Q/c_p\bar{T}_o)$, an order-unity parameter in the distinguished limit defined in Eq. (17). The reaction-rate in (16) provides the characteristic induction time $t_i = B^{-1}\exp\left(E_a/R^o\bar{T}_o\right)$ used in scaling s and n, reducing the heat-release rate to $\Omega = y\exp(\beta\hat{T})$ and the reactant conservation equation (15) to

$$\frac{\partial y}{\partial s} = -\Omega = -ye^{\beta\hat{T}}, \tag{18}$$

where $y = Y/\bar{Y}_u$. The boundary condition for the reactant mass fraction behind the chemically frozen shock reduces to $y = y_u$, where $y_u = Y_u/\bar{Y}_u$ differs from unity for nonuniform incoming composition. Equations (10), (11), (18), and (14) constitute a set of conservation equations for $\hat{T}$, $\hat{p}$, y, and $\hat{V}$. The change of the incident angle $\hat{\sigma} = (\sigma - \bar{\sigma})/q \sim 1$ is an additional variable of the problem, which enters through the boundary conditions at the leading shock. These can be determined by linearizing the Rankine-Hugoniot Eqs. (2), (3), and (5) to give

$$\hat{T} = \hat{T}_u + A_T\hat{M}_u + B_T\hat{\sigma}, \quad \hat{p} = A_p\hat{M}_u + B_p\hat{\sigma}, \quad \hat{V} = A_\nu\hat{M}_u + B_\nu\hat{\sigma} \tag{19}$$

involving the coefficients

$$A_T = \frac{1}{F_T}\frac{\partial F_T}{\partial M_u}, B_T = \frac{1}{F_T}\frac{\partial F_T}{\partial \sigma}, A_p = \frac{1}{F_p}\frac{\partial F_p}{\partial M_u}, B_p = \frac{1}{F_p}\frac{\partial F_p}{\partial \sigma}, A_\nu = \frac{\partial F_\nu}{\partial M_u}, B_\nu = \frac{\partial F_\nu}{\partial \sigma}, \tag{20}$$

to be evaluated at $M_u = \bar{M}_u$ and $\sigma = \bar{\sigma}$. For generality, the jumps described by Eq. (19) account for the possible existence of small fluctuations of order q in the Mach number and temperature of the approaching stream, described by the known order-unity functions $\hat{T}_u = [(T_u - \bar{T}_u)/\bar{T}_u]/q$ and $\hat{M}_u = (M_u - \bar{M}_u)/q$.

The solution simplifies when the post-shock flow is supersonic, i.e. $\bar{M}_o > 1$, condition given for certain values of $\bar{M}_u$ and $\bar{\sigma}$. The Euler equations can be formulated in characteristic form, with three different characteristic curves crossing any given point, i.e. the streamline and the two Mach lines $C_\pm$, crossing the streamline with local angles $\pm\mu$ with $\mu = \sin^{-1}\left(M^{-1}\right)$ [6]. For weakly exothermic detonations, all three families of characteristics are straight lines with fixed inclination angles, be the streamlines $n =$ constant, and Mach lines given by $C_\pm :\ s - n/\tan\bar{\phi}_o$. The condition that the normal component of the velocity behind the shock is subsonic, implies that $\bar{\mu}_o > \bar{\phi}_o$, so that the C_+ characteristics always reach the shock, while the C_- characteristics originate there. The problem can be formulated in characteristic form by combining Eqs. (10), (11) and (14) to give

$$\frac{\partial I^\pm}{\partial s} \pm \frac{1}{\sqrt{\bar{M}_o^2 - 1}}\frac{\partial I^\pm}{\partial n} = \frac{\gamma\bar{M}_o^2}{\bar{M}_o^2 - 1}\Omega \tag{21}$$

for the characteristic variables $I^\pm = \hat{p} \pm \frac{\gamma\bar{M}_o^2}{\sqrt{\bar{M}_o^2-1}}\hat{V}$. Using $\hat{p} = (I^+ + I^-)/2$ in (11) provides

$$\frac{\partial\hat{T}}{\partial s} - \frac{\gamma - 1}{2\gamma}\frac{\partial}{\partial s}(I^+ + I^-) = \Omega, \tag{22}$$

which, together with Eqs. (18), and (21) are the basis for the description of the supersonic post-shock flow in two-dimensional, steady, weakly exothermic detonations. The integration of Eq. (22) along the streamlines

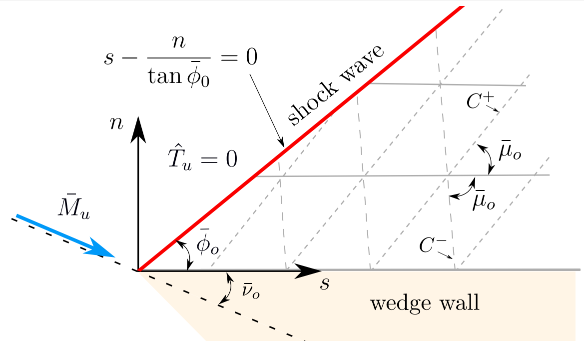

Figure 2: Schematic view of the problem arising in the interaction of a detonation and a wedge wall.

and of Eq. (21) (minus) along the C_- characteristics is initiated at the shock $s = n/\tan\bar{\phi}_o$, where the values of $\hat{T}$ and I^- depend on the value of I^+ reaching the shock from below. The derivation of the post-shock expressions for $\hat{T}$ and I^- begins by using the relations given in Eq. (19) to relate the values of the characteristic variables $I^\pm$ at the shock with the perturbations of upstream Mach number and incident angle

$$I^+ = A^+\hat{M}_u + B^+\hat{\sigma} \quad \text{and} \quad I^- = A^-\hat{M}_u + B^-\hat{\sigma} \tag{23}$$

where

$$A^\pm = A_p \pm \frac{\gamma M_o^2}{\sqrt{M_o^2 - 1}} A_\nu \quad \text{and} \quad B^\pm = B_p \pm \frac{\gamma M_o^2}{\sqrt{M_o^2 - 1}} B_\nu. \tag{24}$$

The first equation in (23) can be used to provide $\hat{\sigma} = -(A^+/B^+)\hat{M}_u + (1/B^+)I^+$ for the local incident angle as a function of the value of I^+ reaching the shock from below. Which used in (19) and (23) yields the expressions relating the post-shock values of $\hat{T}$ and I^- with I^+,

$$\hat{T} = \hat{T}_u + \left(A_T - \frac{B_T}{B^+}A^+\right)\hat{M}_u + \frac{B_T}{B^+}I^+, \qquad I^- = \left(A^- - \frac{B^-}{B^+}A^+\right)\hat{M}_u + \frac{B^-}{B^+}I^+. \tag{25}$$

4 Sample Computations

As an illustrative example, the above formulation is used to analyze the establishment of an oblique detonation at a wedge, defined by a given deflection angle. With the origin of the reference frame located at the impingement point, as indicated in Fig. 2, the solution involves a reflection condition at the wall $n = 0$, such that no flux can traverse the wedge $\hat{V} = 0$, or in the characteristics formulation $I^+ = I^-$. The problem reduces to the integration of Eqs. (21), (22), and (18) with initial values $\hat{T} = \frac{B_T}{B^+}I^+$, $I^- = \frac{B^-}{B^+}I^+$, $y = 1$ at the shock $s = n/\tan\bar{\phi}_o$ and of Eq. (21) with the initial value of $I^+ = 0$. Sample temperature distributions are plotted in Fig. 3 for $\bar{M}_u = 2.5$, $\sigma = 50^{\circ}$. The calculations reveal changes in the character of the solution associated with increasing values of the activation energy β, with the smooth transitions found for small values of β being replaced by cell-like oscillatory structures for larger values of β, reminiscent of the cellular structures observed in wedge-induced problems [4]. Eventually leading to the formation of a triple point at the leading shock, as β increases.

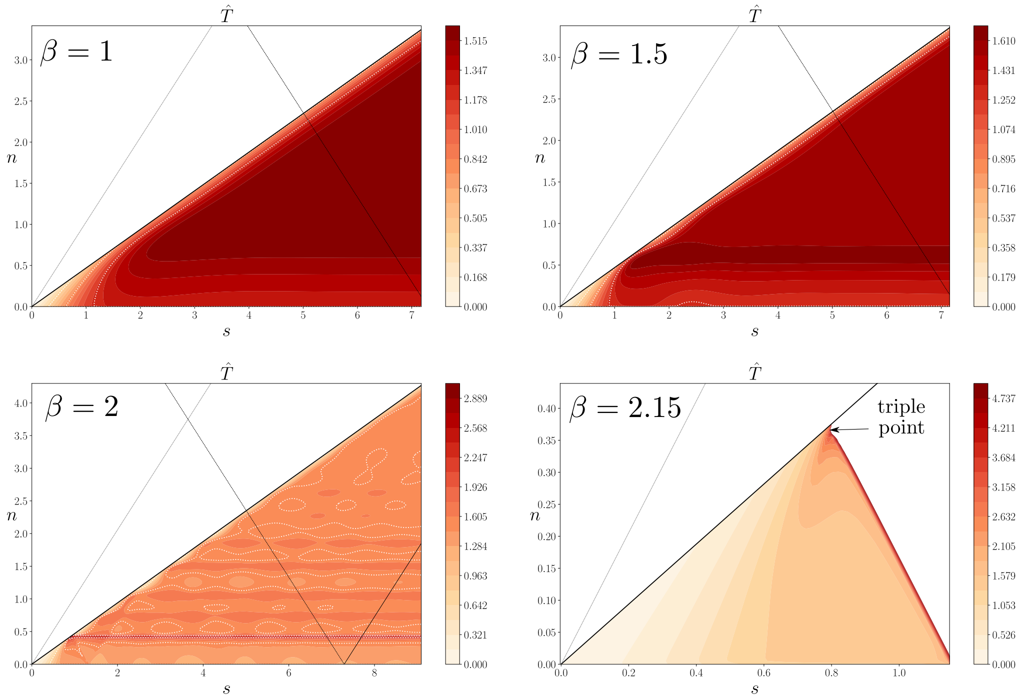

Figure 3: Temperature distributions behind the shock for a detonation with $\bar{M}_u = 2.5$ and $\sigma = 50^o$. Note that different domains are considered to correctly depict each steady solution.

Acknowledgments

The work of DMR and CH was supported by the Spanish Ministry of Science through grant # ENE2015-65852-C2-1-R) and by the Fundación Iberdrola España through grant # BYNV-ua37crdy. The work of ALS and FAW was supported by the US AFOSR Grant No. FA9550-16-1-0443.

References

[1] K. Kailasanath, "Review of propulsion applications of detonation waves," *AIAA journal*, vol. 38, no. 9, pp. 1698–1708, 2000.

[2] C. Huete, A. L. Sánchez, F. A. Williams, and J. Urzay, "Diffusion-flame ignition by shock-wave impingement on a supersonic mixing layer," *Journal of Fluid Mechanics*, vol. 784, pp. 74–108, 2015.

[3] C. Huete, A. L. Sánchez, and F. A. Williams, "Diffusion-flame ignition by shock-wave impingement on a hydrogen–air supersonic mixing layer," *Journal of Propulsion and Power*, pp. 256–263, 2016.

[4] C. Li, K. Kailasanath, and E. S. Oran, "Detonation structures behind oblique shocks," *Physics of Fluids*, vol. 6, no. 4, pp. 1600–1611, 1994.

[5] F. A. Williams, *Combustion theory*. Cummings Publ. Co, 1985.

[6] W. D. Hayes, R. F. Probstein, and R. R. Probstein, *Hypersonic inviscid flow*. Courier Corporation, 2004.